

WIND FARM REPOWERING GUIDED BY VISUAL IMPACT CRITERIA

Cristina Manchado^{1*}; Valentin Gomez-Jauregui¹; Piedad E. Lizcano¹; Andres Iglesias²; Akemi Galvez²; Cesar Otero¹.

¹ R&D EgiCAD, School of Civil Engineering, Universidad de Cantabria, Avda. de los Castros s/n, 39005, Santander, Cantabria. Spain.

² Department of Applied Mathematics and Computational Sciences, School of Civil Engineering, Universidad de Cantabria, Avda. de los Castros s/n, 39005, Santander, Cantabria. Spain.

* Corresponding author: manchadoc@unican.es

ABSTRACT.

Within a repowering context, this paper opens a new field of application for visibility and Visual Impact Assessment (VIA) procedures in the decision-making process typical of the design stage of Wind Farms (WF). The proposed methodology presents a test capable of reporting on the visual sustainability of different layouts. It is called Equivalent Visual Impact (EVI). To work with EVI, visibility data have to be numerically available at a level of each pixel and each Wind Turbine (WT). This is called High Resolution Data (HRD). The paper shows how these ideas, EVI and HRD, were applied to a real repowering experience; the result was that the WF could sustain an increment in its power by 37.25 % with no additional visual effects. Other associated consequences are discussed.

Keywords: Equivalent visual impact, EVI, Level of detail, Visual impact assessment, VIA, wind energy repowering

1.Introduction.

This article reports a study of Wind Farm (WF) repowering¹ guided by visibility and Visual Impact Assessment (VIA) criteria. The proposed methodology introduces a new condition capable of addressing the decision-making process carried out during the design stage: we call this condition the Equivalent Visual Impact (EVI). To take advantage of this methodology, visibility data (mainly visibility maps and viewsheds) have to be numerically displayed at a definition level of each pixel and each Wind Turbine (WT). This is what we name High Resolution Data (HRD). Both EVI and HRD will be more precisely described in section 3.5.

Actually, within a repowering context, the paper opens a new field of application for VIA procedures in the decision-making process at the design stage of WFs. Very few background scientific reports connect repowering and VIA [1]; and they are focused on planning at a regional or national level. The relevant role that VIA can play in the Environmental Impact Assessment report stage is well known; but including visibility and VIA issues when the WF design is still in progress is something that has not been addressed up to now. However,

¹ *The situation does not correspond exactly with a repowering case since the WF has not been erected yet. However, stakeholders and regional authorities always refer to this proposal as a repowering case, therefore we have decided to keep this term.*

including visibility and VIA criteria within the Decision Support System (DSS) when defining the layout of a WF should be understood as a need (maybe even as a must). This is one of the of the main contributions of the paper, in particular this article describes a way to deal with visual indicators in similar terms to (or together with) other relevant data, such as the wind resource, the terrain relief, the ways of extracting the generated power, etc.

This work arises from a real development. A WF already authorised but not yet erected was submitted for a new repowering authorisation, carried out by means of updating the model of their turbines (actually taller than the original ones). The presumed increment of visual intrusion was calculated and compared with the initial design. A detailed analysis of the visual effects at both pixel level and turbine level permitted the designer to propose a set of suitable mitigation measures, either: i) removal of some turbines, ii) vegetation barrier erection at a long distance from the observer, or iii) displacement of one or several wind turbines (WTs). As a result, the WF was repowered in such a manner that its relative visual effect was not increased (“relative” in the sense of compared with the initial situation, which was already authorised). Everything was numerically processed, which additionally enabled it to be justified (to stakeholders and population) with rigor, precision and objectivity.

The paper is developed as follows: section 1.1 presents and explains the meaning of the indicators selected in this research for carrying out the visual assessment; section 1.2 provides a more detailed review on VIA and visibility indicators. Section 1.3 considers the viability of using techniques of optimization. Section 2 features the problem. Section 3 details the methodology and, in particular, defines both the HRD and EVI concepts. Section 4 clarifies the rationale of the iterative process in the search for convergence of values leading to the EVI condition. In section 5 the methodology is discussed. Section 6 presents the conclusions and future works.

1.1. Visibility indicators used in this work. Overall and local visual effects.

The present work is based on two indexes suitable to describe conditions of visual intrusion.

The first index is called MVE (Magnitude of the Visual Effect) [1]. It was originally created to describe overall visual effects (at a regional level) in the visual inventory. MVE is the product of three visual indicators: visually affected area, visually affected population and visual exposure in linear stretches (expressed either as travel time or as distance).

Indicator of visually affected area analyses the layer of population nuclei in the domain of study and gives the total amount of surface area proved to be visible from the set of WTs being analysed; it is expressed in m² or km². The indicator of visually affected population works over the layer of population in the domain of study. It is generally made up by a layer of pixels, each one of them having associated the value of the population living inside; this indicator is expressed in number of inhabitants. The visual exposure in linear stretches works over the layer of roads by selecting the subset of them having visibility over the set of WTs being analysed; this indicator is expressed in meters or kilometres.

In MVE, the condition “to be visible from the set of WTs” needs to be precisely defined. The most restrictive criterion establishes that for an area (or a pixel or a road stretch) to be visually affected it must have at least one visible pixel. Some other less restrictive criteria can be easily formulated. The index MVE was initially proposed in the study for the Wind energy development in Cantabria (Spain) [1]. Since 2014 this index has been included in the regional regulation for the renewable energy development in Cantabria [2].

The second index is called the Spanish Method (SPM) [3]. SPM gathers 5 indicators called *a*, *b*, *c*, *d* and *e*. The method was thought to be used for the Visual Impact Assessment of only one WF over a single population area. Thus, SPM is suitable for measuring local effects. The indicator *a* gives an average value of the number of WTs seen from the population nucleus (visibility to the WF). The indicator *b* gives the ratio of surface area of the population nucleus visually affected by the WF (visibility from the WF). The indicator *c* gives an estimation of the visual effect of the WF over the population nuclei when its relative position (in front, in diagonal or in lateral) is considered; this value is weighted by the effect of the total number of WTs of the WF. The indicator *d* gives an estimation of the distance decay effect. Finally, the indicator *e* gives a value of the effect of the visibility depending on the amount of visually affected population.

SPM was analysed and modified in [4], where an improved version of this index was completely reformulated under the name of SPM2 (Spanish Method 2). Apart from other features, SPM2 makes it possible to fully program the methodology, giving as a result a set of five indicators fully replicable. Additionally, in this new version SPM2 can be applied to any element of the visual inventory, not only over population nuclei.

Depending on the particular conditions of each project, some indicators of SPM2 perform better than others. In this case, indicator *b* of SPM (or SPM2) proves to be analogous to the visually affected area of MVE. Indicator *c* is not a good reference in this study due to the disperse distribution of the layout. The value of indicator *d* is always maximum in this study, due to the values of the thresholds agreed by stakeholders (see section 2.3). Finally, in our case indicator *e* is not useful provided that population remains the same under all our hypotheses of repowering (see further details throughout the section 4). Consequently, SPM2 can be reduced to indicator *a*.

Working together, MVE and *a* clearly describe very well the status of visual load of the area of study: on the one hand, indicator *a* depicts local effects and MVE accounts for overall effects; on the other hand, indicator *a* depicts the amount of WTs seen from the visual inventory elements of study (viewer's approach) while the MVE index summarizes the number of pixels having visibility (total or partial) of the WF (affected territory approach). Indicator *a* was computed at a pixel level according to the next expression:

$$a = \frac{\sum \text{WT seen in each pixel of the area}}{\text{Total number of WTs in the WF}} \quad [\text{eq. 1}]$$

This expression is applied to the whole set of pixels of the layer of the visual inventory under analysis

1.2. Visibility indicators in literature.

Indicators MVE and *a* used in this work were respectively published in [1] and [3]. These works are strongly related to references [5], [6] and [7]. In [5], Rodrigues et al. proposed a methodology for the assessment of visual impact at different territorial analysis levels (local, regional or national) and for different renewable technologies by means of four indexes: visually-affected area, visually-affected populated area, visually-affected travel time and estimated visual perception. In [6], Kokologos et al. presented a methodology for the aesthetic integration of a large-scale WF based on a combination of SPM indicators [5] with 3D simulation techniques. Tsousos [7] applied SPM to a WF erected on a Greek island and contrasted and validated the method.

Some other authors have also developed studies related to visual or visibility indicators: McAulay [8], Bishop [9], Hagerhall et al. [10], Bishop and Miller [11], Ladenburg and Dubgaard [12], Ladenburg [13], Möller [14], Torres-Sibille et al. [15], Ladenburg and Möller [16], Molina-Ruiz et al. [17], Dentoni and Massacci [18], Kapetanakis et al. [19], Fernández-Jimenez et al. [20], Wróżyński et al. [21] and Sunak and Madlener [22]. Together, all the references in this section show a total of 54 visual indicators. Not all of them are really different. In figure 1, we have summarised the coincidences giving as a result a total of 17 really different indicators. This figure not only suggests the possibility of applying the methodology presented in section 3 to other indicators but also proves that those used in this communication are frequently considered by authors in the specialised literature.

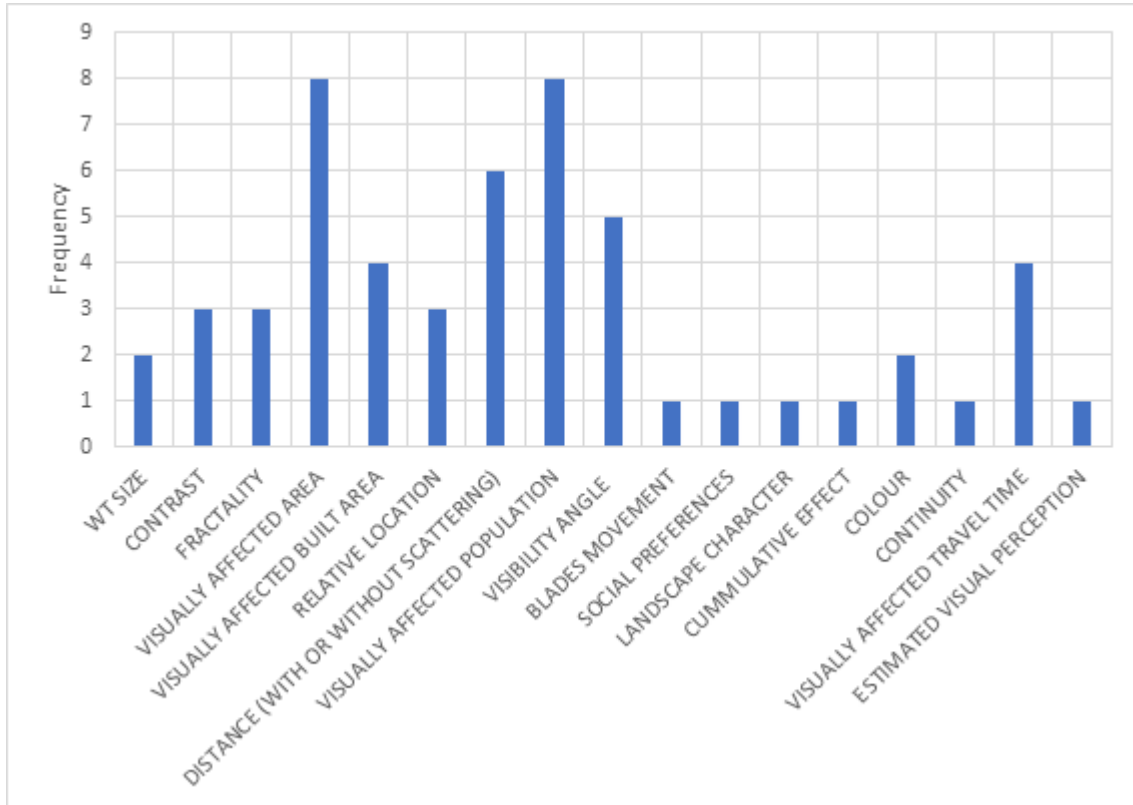


Figure 1: Visibility and visual indicators used by different authors in the field of VIA (Visual Impact Assessment) and LIA (Landscape Impact Assessment).

1.3. Optimization versus decision-making strategies.

The owner of the project obtained the layout of the initial WF by means of an optimization process combining factors such as the wind resource, the accessibility of the terrain, WT costs, WT erection and energy evacuation costs. In this current work, the most restrictive repowering condition was to avoid any increment of visual impact, so optimization problem cannot be formulated simply in terms of maximizing the exploitation of the wind resource. Undoubtedly, such strategy would lead to select new alternative layouts in places that would elicit a higher visual impact, which would lead the project to failure. Stakeholders decided to give the original layout the condition of unalterable (see section 2.3), this meaning that WTs could be removed or repowered but not displaced.

Then the problem of repowering was considered according to two different strategies: the first one would be based on the search of a suitable decision supported making process and the other one would be based on optimization techniques maximizing benefits but keeping bounded the visual effects.

The first strategy is the real goal of this contribution and is fully developed in the next sections. The second one is out of the scope of this paper and hence, it is only briefly summarized in this section (see Figure 2).

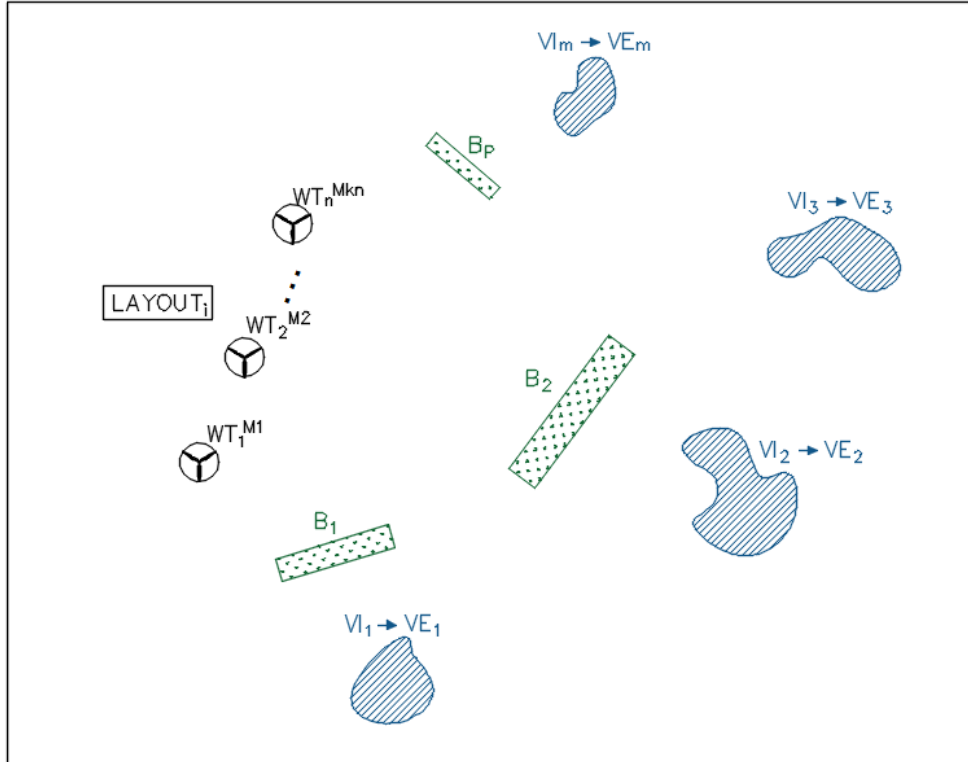


Figure 2: A representation of the optimization of the WF energy benefits conditioned to the minimization of the visual effects. WT_j^{Mkj} represents a wind tower erected using the model of turbine M_k ; B_i represents a vegetal barrier and VI_i represents an element of the visual inventory.

Let us consider:

- a wind farm $WF = \{WT_1, WT_2, \dots, WT_n\}$.
- a set of k possible different available models of wind tower $\{M_1, M_2, \dots, M_k\}$. Each model M_i has its own set of properties (size, power, blades diameter, etc.). A wind tower WT_i using the model M_j is denoted as WT_i^{Mj} . This notation also allows to include a M_0 (model 0) to represent the removal of a wind turbine: WT_i^{M0} . Thus, M_0 symbolizes a model having size = 0, power = 0, etc.
- Consequently, a particular hypothesis of layout can be denoted as:

$$LAYOUT_k = \{WT_1^{Mk1}, WT_2^{Mk2}, \dots, WT_j^{Mkj}, \dots, WT_n^{Mkn}\}$$

where WT_j^{Mkj} means that the wind tower WT_j implements the model M_{kj} , selected from the set $\{M_0, M_1, M_2, \dots, M_k\}$.

- a set of m elements of the visual inventory $VI = \{VI_1, VI_2, \dots, VI_m\}$. According to previous sections, the visual effect of WF over VI can be expressed by means of the value of one of the indicators shown in section 1.2. This gives rise to a new set $VE =$

$\{VE_1, VE_2, \dots, VE_m\}$, where each VE_i is the value of the chosen visual indicator VE_i and for a particular configuration $LAYOUT_i$.

- According to this, VE represents the visual cost of the $LAYOUT_i$ over the visual inventory VI .
- Eventually, to reduce the value VE , a set of vegetal visual barriers $VB = \{B_1, B_2, \dots, B_p\}$ can be considered. Each barrier B_i is a binary variable taking value 0 (non erected) or 1 (erected).

Under these conditions, the problem can be stated as:

$$\min_{\bar{x}} F(\bar{x})$$

where $F(\bar{x})$ is the objective function, and $\bar{x} = (x_1, x_2, \dots, x_r)$ represents the list of design variables. In our particular case, the objective function is given by the total cost of energy, TCOE, defined as:

$$TCOE = \alpha \cdot LCOE + \beta \cdot VCOE \quad [\text{eq. 2}]$$

where LCOE represents the levelized cost of energy (defined as either in [23] or in [24]) and VCOE represents the visual cost of energy, explained below. The parameters α and β are used to modulate the different contributions of terms LCOE and VCOE to the final TCOE. The visual cost function, VCOE, is defined as:

$$VCOE = \sum_{j=1}^m (VE_j - \sum_{i=1}^p \lambda_i \theta_{ij}) \quad [\text{eq. 3}]$$

where θ_{ij} is a binary variable returning 1 if visual barrier B_i contributes to mitigate the visual effect VE_j and 0 otherwise, and λ_i quantifies the value of such an impact (if any). Note that the visual effect can be computed according to [eq. 1].

Therefore, the optimization problem becomes:

$$\min_{\bar{x}} TCOE(\bar{x}) \text{ subjected to } VE_j \leq VEL_j \quad (j=1, \dots, m)$$

This is a nonlinear optimization problem that can be solved by either classical mathematical optimization techniques [23] or through evolutionary techniques [25]. Finally, note that additional constraints can also be imposed on this model as either equalities or inequalities. They can be addressed by either mathematical optimization techniques such as the Karush-Kuhn-Tucker (KKT) approach (provided that some regularity conditions are satisfied) or through numerical multiobjective optimization techniques for ill-conditioned or conflicting constraints".

2.The case study.

2.1.Description.

The original WF was made up of 34 WTs. It would be erected somewhere in the Atlantic coastland (see figure 3)². Nonetheless, the time lapsed for authorisation was so long that the original turbines ran the risk of becoming obsolete. Given that current turbines could be more powerful, the promoter suggested the possibility of incrementing the WTs' power, while maintaining their position exactly as it was in the original (and already approved) project. Thus, this change could affect the height but not the position, nor the overall layout.

During the new stage of meetings prior to the project for repowering authorisation, the regional administration obliged a guarantee that the new design would not involve an increase in the visual effects, compared to those in the initial proposal. However, an enlargement in the size of the towers would presumably involve an increment in visibility: initially affected areas would suffer a greater visual intrusion whereas other areas not initially affected could become so.

The visual inventory (see more detail in section 2.4) in the area of study was the same in both the original and the repowering situations. According to the sensitivity expressed by several social groups, the protection of a selected set of historical and cultural places was compulsory. More precisely, the stakeholders agreed that four highly relevant elements had to be completely protected from any increment of visual effects. These elements, shown in figure 3, were: i) a high value landscape area (area 1), ii) a monumental population nucleus (area 2), iii) a historic site (area 3) and iv) a cultural itinerary (line 1) particularly meaningful for local populations and of great interest for visitors.

² The promoter allows to publish this paper under the premise that no specific details of the park would be disclosed unless absolutely necessary.

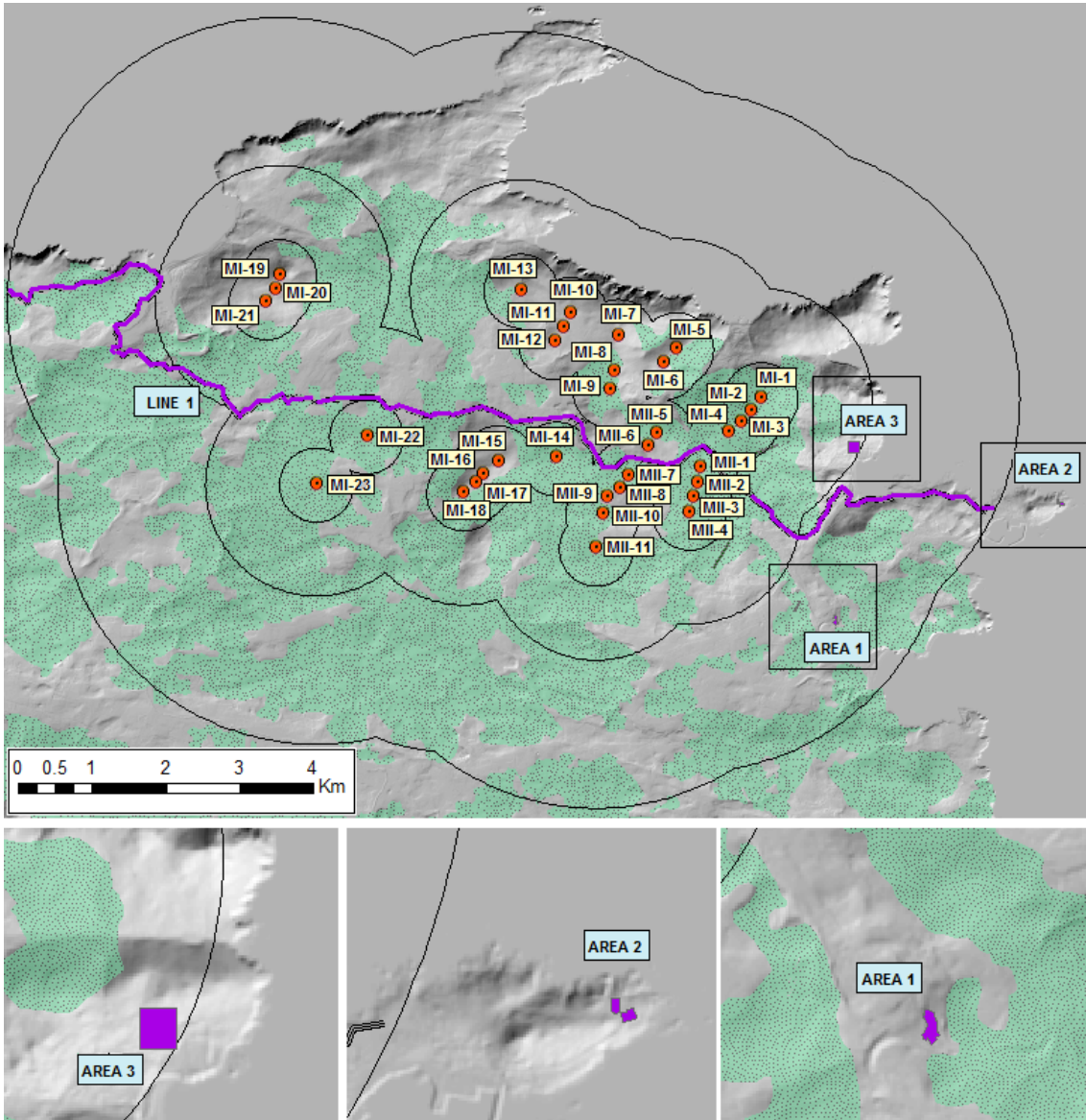


Figure 3: WF's layout. Above: the four elements of the visual inventory are labelled as area 1, area 2, area 3 and line 1. The outer black line is the distance threshold buffer. The other inner black lines are distance references at 500 m and 1500 m. Vegetation (green polygons) are also shown in dotted areas. Below: larger images of the three critical areas (visual inventory).

2.2. Authorisation conditions.

According to the considerations summarised in the previous section, the regional authorities stated that a repowering proposal would result acceptable if:

1. Overall visual effects were not greater than the ones yielded by the original WF and
2. Four critical elements of the visual inventory (areas 1, 2, 3 and line 1) did not suffer any increment of visual intrusion.

2.3. Landscape and visual specifications.

Consequently, the new study of VIA was carried out according to these conditions and assumptions:

- The position of the WTs should remain unchanged before and after repowering the WF. This means that any WT could be removed but not displaced.
- The original landscape character and the definition of the landscape quality areas should be equal in both cases, before and after repowering.
- Maintaining the short-distance visual effects unchanged was a priority. The visual thresholds were established from 0 to 3500 meters.
- Viewsheds were calculated considering the maximum height of the turbine (tower and blades) and the existing vegetation. An average height of vegetation of 15 meters was set (a conservative value for the area).
- Mitigation by WT removal was acceptable.
- Mitigation by remote vegetal barrier erection [1] [26] was admissible.
- For barrier mitigation purposes, the average vegetation height was set to 25 meters.
- The overall visual impact had to be obtained by means of the MVE index [1], as the product of the indicator of visually affected area and the one of visual exposure expressed as linear stretches visually affected.
- To complement MVE, the local visual impact for areas 1, 2, 3 and line 1 had to be obtained by means of indicator α of the SPM2 method [4].

The VIA computational tool was MOYSES [26] [27] [28].

2.4. Input Data

- Digital Terrain Model: DTM of 10-meter pixel size, obtained from 2014 PNOA LIDAR FLIGHT (National Plan of Aerial Orthophotography).
- Visual inventory: the four elements considered (areas 1, 2, 3 and line 1) were extracted from the official regional cartography. From this model, area 1 (5112 m²) contained 60 pixels, area 2 (3740 m²) contained 46 pixels, area 3 (20653 m²) contained 224 pixels and line 1 (18583 m) was modelled as a line discretised as a set of 17060 pixels.
- Vegetation: polygons were extracted from Corine Land Cover (scale 1:100,000). Code values 311, 312 and 313 were used for the selection filter. They correspond to natural vegetation in open spaces (broad-leaved forest, coniferous forests and mixed forests). The density of vegetation existing in the area of study was really high (see figure 3).
- WT types:
 - Model 1, with 67 meters hub height, 66 m rotor diameter and 1650 kW power, used for the original hypothesis.
 - Model 2, with 93 meters hub height, 106 rotor diameter and 2500 kW power, used for the repowering hypotheses.
 - Model 3, with 78 meters hub height, 80 m rotor diameter and 2000 kW power, only used for hypothesis 5 (see section 4.1.6).
 - Model 4, with 67 meters hub height, 66 m rotor diameter and 2000 kW power. Having the same nominal power, this model is less efficient than model 3.

The promoter proposed this set of new possible models to be considered and checked the layout in order to preserve always the minimum separation distance between turbines.

3. Methodology.

3.1. Starting situation.

The starting situation (hypothesis 0) is the original layout with 34 WTs of model 1 (section 2.4) 67 m. tall. The repowering situation considers the same layout, but erected using model 2, 93 m. tall. Hypothesis 1 is expected to elicit an increment of visual intrusion. This will give rise to a systematic decision-making process in order to create more new repowering hypotheses able to mitigate this visual intrusion to acceptable values (section 2.2).

3.2. Measuring visual effects.

As previously said, the measurement of visual effects is carried out through the comparison of the MVE index (overall effects) and indicator a of SPM2 (local effects). As an illustration, table 1 shows the contrast between hypothesis 0 and 1 for MVE and table 2 does so for indicator a . In section 4.1 both tables will be presented with the set of values obtained in the whole series of assessed hypotheses.

Table 1: Pattern of information for MVE (Magnitude of Visual Effect) index.

MVE (affected area x affected length)	Visibility area (km ²)	Visibility length(km)	MVE product (km ³)
Hypothesis 0 (Original Layout)	0.0061	11.64	0.0710
Hypothesis 1	0.0067	12.22	0.0819

Table 2: Pattern of information for indicator a of SPM2 (Spanish Method 2) for hypotheses 0 and 1.

INDICATOR a	Area 1	Area 2	Area 3	Line 1
Hypothesis 0 (Original Layout)	0.1590	0.0010	0.0000	0.1012
Hypothesis 1	0.3001	0.0020	0.0009	0.1181

3.3. High Resolution Data (HRD)

Table 3 is an excerpt of the HRD status of an element of the visual inventory (more precisely, of the area 1). Each row represents a pixel and each column represents a WT. In each cell (i,j) a null value is assigned if pixel i does not have visibility of WT j . Otherwise, instead of saving a value of 1, the distance from the centre of the pixel to the WT is recorded. This simple procedure makes it easier to apply distance threshold filters; finally, it becomes clear that: i) a row full of null values depicts a pixel free of visual intrusion; ii) a column full of null values represents a WT causing no visual effect on the viewer (e.g., WTG02, WTG06, and WTG07 in this table).

The right column in table 3 (visible WTs) shows the number of wind turbines seen from each pixel. The bottom row (visible pixels) shows the number of pixels visually affected by each WT. Table 3 holds enough information to calculate the value of indicator a . See [eq.1] in section 1.1). According to it, $a = 67/11 = 6.09$ WTs. This value means that, on average, 6.09 WTs are seen. It is usual to express the value of the indicator a in the range $[0, 1]$, it is, $6.09 / 11 =$

0.554. This means that, on average, a 55.4% of the WTs of the WF are seen from the considered area of study.

Table 3: Status of visibility for pixels of the area of study (rows) and wind turbines of the wind farm (columns). Hypothesis 0. A cell worth 0 has no visibility; a visible cell stores the distance between the wind turbine and the pixel. The last row shows the visible pixels for each wind turbine. The rightmost column shows the visible wind turbines from each pixel.

WT pixel	WTG01	WTG02	WTG03	WTG04	WTG05	WTG06	WTG07	WTG08	WTG09	WTG10	WTG11	VISIBLE WTs
0	0	0	2913	0	3433	0	0	3480	0	2527	2625	5
1	0	0	0	0	3438	0	0	0	0	0	2632	2
2	0	0	0	3334	3406	0	0	0	0	0	2569	3
3	0	0	0	3336	3410	0	0	0	0	2483	2576	4
4	0	0	2857	3339	3414	0	0	0	2401	2489	2583	6
5	5114	0	2866	3342	3418	0	0	3443	2407	2496	2590	8
6	5118	0	2875	3344	3422	0	0	3450	2413	2502	2597	8
7	5133	0	0	0	0	0	0	3479	2436	2528	2625	5
8	5137	0	0	0	0	0	0	0	2442	2535	2632	4
9	5141	0	0	0	0	0	0	0	2448	2542	2639	4
10	0	0	0	0	3451	0	0	0	2454	2548	2646	4
11	0	0	2845	3343	3415	0	0	3429	2398	2484	2576	7
12	0	0	2854	3346	3419	0	0	3436	2403	2491	2583	7
VISIBLE PIXELS	5	0	6	7	10	0	0	6	9	11	13	67

3.4. Setting a new mitigation hypothesis based on HRD local effects.

Let us suppose that the status shown in table 3 corresponds to our starting situation (hypothesis 0) and that we are testing a new hypothesis i , characterised by the values shown in table 4. The value for indicator a is $84 / 11 = 7.64$. Hypothesis i seems to be not a good solution, since the value of indicator a has increased by 25.45% from its original one (7.64 / 6.09).

Table 4: Status of visibility for pixels of the area of study (rows) and wind turbines of the wind farm (columns). Hypothesis i represents a generic situation.

WT pixel	WTG01	WTG02	WTG03	WTG04	WTG05	WTG06	WTG07	WTG08	WTG09	WTG10	WTG11	VISIBLE WTs
0	0	0	2913	0	3433	0	0	3480	0	2527	2625	5
1	0	0	0	0	3438	0	0	3339	0	0	2632	3
2	0	0	0	3334	3406	0	0	3342	0	0	2569	4
3	5100	0	0	3336	3410	2583	0	3344	0	2483	2576	7
4	5110	0	2857	3339	3414	2590	0	0	2401	2489	2583	8
5	5114	0	2866	3342	3418	2597	0	3443	2407	2496	2590	9
6	5118	0	2875	3344	3422	0	0	3450	2413	2502	2597	8
7	5133	5248	0	0	0	0	0	3479	2436	2528	2625	6

8	5137	5258	0	0	0	0	2528	0	2442	2535	2632	6
9	5141	5270	0	0	0	0	2535	0	2448	2542	2639	6
10	0	5290	0	0	3451	0	2542	0	2454	2548	2646	6
11	0	5295	2845	3343	3415	0	2548	3429	2398	2484	2576	9
12	0	0	2854	3346	3419	0	0	3436	2403	2491	2583	7
VISIBLE PIXELS	5	0	6	7	10	0	0	6	9	11	13	84

The suggested procedure is as follows: table 5 offers a HRD representation of the difference in visibility status between hypothesis i and hypothesis 0. In this table, pixels worth 0 do not undergo any additional visual alteration. Indeed, in hypothesis i they have the same value as the one in hypothesis 0. Thus, the designer can concentrate the effort on the positive differences³ shown in table 5.

The bottom row of table 5 shows the accumulated number of non null cells for each WT. These amounts can be represented on a graph. See figure 4: in hypothesis i , WTs 03, 04, 05, 09, 10 and 11 show the same visual conditions as the ones in hypothesis 0. The designer could decide to focus the new hypothesis on acting on the machines WT 01, 02, 06, 07 or 08. For example, reducing their height or setting up a mitigation barrier. This would lead to a new hypothesis that, compared with hypothesis 0, would give a new table of differences and a new synthesising graph similar to the one shown in figure 4.

This strategy will be iteratively applied next in section 4 to solve the formulated repowering problem. This way to work with tables 3, 4, and 5 opens a way to obtain a reduction in the value of indicator a that can guarantee the authorisation conditions of repowering (see section 2.2).

Table 5: Table of values (hypothesis i – hypothesis 0). Each cell shows the difference between the correspondent visibility values in tables 3 and 4.

WT	WTG01	WTG02	WTG03	WTG04	WTG05	WTG06	WTG07	WTG08	WTG09	WTG10	WTG11
pixel											
0	0	0	0	0	0	0	0	0	0	0	0
1	0	0	0	0	0	0	0	3339	0	0	0
2	0	0	0	0	0	0	0	3342	0	0	0
3	5100	0	0	0	0	2583	0	3344	0	0	0
4	5110	0	0	0	0	2590	0	0	0	0	0
5	0	0	0	0	0	2597	0	0	0	0	0
6	0	0	0	0	0	0	0	0	0	0	0
7	0	5248	0	0	0	0	0	0	0	0	0
8	0	5258	0	0	0	0	2528	0	0	0	0
9	0	5270	0	0	0	0	2535	0	0	0	0
10	0	5290	0	0	0	0	2542	0	0	0	0
11	0	5295	0	0	0	0	2548	0	0	0	0

³ Negative differences can exist. This is usual when mitigation by vegetal barriers is proposed. See sections 4.4 and 4.5, later in this paper.

12	0	0	0	0	0	0	0	0	0	0	0
DIFFERENCES: Hyp i – Hyp 0	2	5	0	0	0	3	4	3	0	0	0

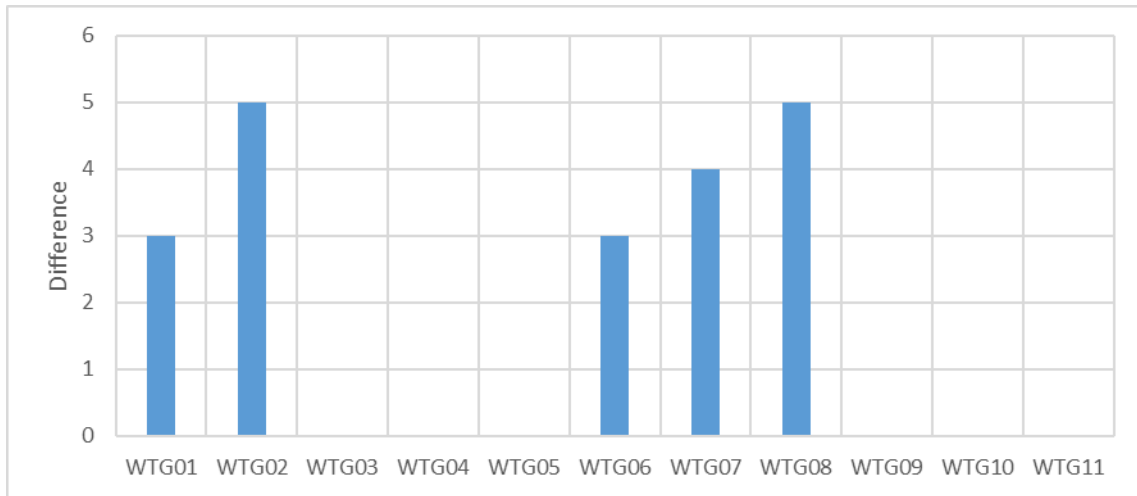


Figure 4: Graphic interpretation of the effects produced in hypothesis i versus hypothesis 0. Turbines 01, 02, 06, 07 and 08 have different visual conditions.

3.5. The Equivalent Visual Impact (EVI) condition.

As indicated in section 1, we are proposing a new condition called Equivalent Visual Impact (EVI). In the same visual inventory, two alternative WF designs observe an EVI condition if a set of selected visual indicators have the same value in both cases. In our case, the EVI condition has been formulated according to these conditions:

- Index MVE has to be the same in both hypotheses (overall visual impact).
- Indicator *a* has to be the same in both hypotheses for Area 1 (local impact).
- Indicator *a* has to be the same in both hypotheses for Area 2 (local impact).
- Indicator *a* has to be the same in both hypotheses for Area 3 (local impact).
- Indicator *a* has to be the same in both hypotheses for Line 1 (local impact).

The condition “to be the same” should accept a tolerance. In this particular case, it was set to 0.001 units for each indicator. The EVI process has an iterative nature, in which the designer usually tests different visual mitigation hypotheses. Each step in this iteration leads to a summary status like the one shown in table 5 and figure 4. The analysis of these data, particularly the graphic ones, helps the designer to make a suitable new proposal in order to achieve the desired EVI condition.

4. Iterative analysis and decision-making.

4.1. Hypothesis 0 and 1.

Hypothesis 0 represents the original layout (using WT model 1, see section 2.4). Hypothesis 1 represents the whole WF repowered (using WT model 2). The corresponding rows in tables 6 and 7 show that the repowering involves an increment of index MVE (0.0819 versus 0.0710), an increment of indicator *a* in area 1 (0.3001 versus 0.1590) and an increment of indicator *a* in line 1 (0.1181 versus 0.1012). Areas 2 and 3 are practically preserved from visual effects from

the WF (the values of indicator α are in both cases practically null). Additionally, there is a local EVI condition in both areas 2 and 3 because the differences of corresponding values in both hypotheses are lower than or equal to 0.001, which is the tolerance value.

Table 6: Values of indicator MVE (Magnitude of Visual Effect) for the different hypotheses.

MVE (affected area x affected length)	Visibility area (km ²)	Visibility length(km)	MVE product (km ³)
Hypothesis 0 (Original Layout)	0.0061	11.64	0.0710
Hypothesis 1	0.0067	12.22	0.0819
Hypothesis 2	0.0067	9.84	0.0659

Table 7: Values of indicator α of SPM2 (Spanish Method 2) for the different hypotheses.

INDICATOR α	Area 1	Area 2	Area 3	Line 1
Hypothesis 0 (Original Layout)	0.1590	0.0010	0.0000	0.1012
Hypothesis 1	0.3001	0.0020	0.0009	0.1181
Hypothesis 2	0.3290	0.0020	0.0009	0.1005
Hypothesis 3	0.2261	0.0019	0.0009	0.0950
Hypothesis 4	0.1894	0.0019	0.0009	0.0987
Hypothesis 5	0.1812	0.0019	0.0009	0.0987
Hypothesis 6	0.1564	0.0018	0.0009	0.0985

In this first step, the EVI condition was not achieved at the overall level. This supported the idea that the methodology shown in section 3.4 should not be applied yet. Instead, for the overall level, the visibility effects of line 1 were predominant (Line 1 is 17060 pixels long, whereas the cumulative area of the rest of the elements reached a value of 324 pixels). This consideration led to focusing the analysis on the visually affected length of line 1. Expressed for each WT, the visual effect is presented in figure 5. It revealed that WTs MI19, 20 and 21 clearly caused the maximum visual intrusion. This led to the establishment of hypothesis 2, with the removal of these machines.

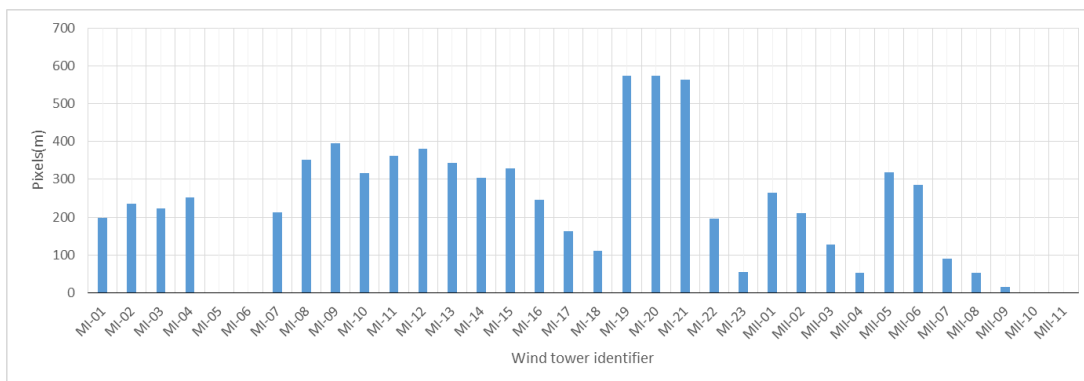


Figure 5:Hypothesis 1: visually affected pixels on line 1 for each wind turbine.

4.2.Hypothesis 2. Removal of MI19, 20 and 21.

Under hypothesis 2 (see the corresponding row in table 6) the EVI condition for the indicator MVE was fulfilled (0.0659 versus 0.0710), which meant that the problem was solved at the overall level. Moreover, at a local level (indicator a , see table 7), three of the four elements of the visual inventory (areas 2, 3 and line 1) also fulfilled the equivalence condition (Line1, whose indicator a was 0.1005, fulfilled it in this hypothesis). Conversely, area 1 remained far from the EVI condition (an indicator a value of 0.3290 compared to 0.1590 in hypothesis 0).

Figure 6 shows in detail the comparison of the visual effects for hypotheses 2 and 0. A total of 21 WTs caused the same visual effect before and afterwards, which meant that their repowering was visually neutral. In consequence, the designer decided to analyse hypothesis 3, applying a change (WT model 3) to 10 WTs: MI01, 04, 15, 16, 17, 18, MII05, 07, 10 and 11.

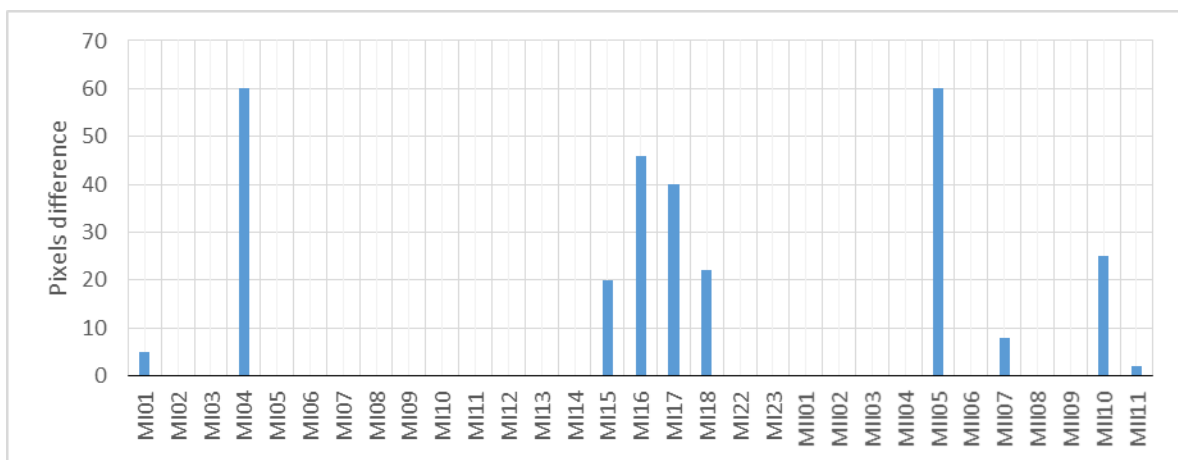


Figure 6: Comparative effect of the pixel difference between hypotheses 2 and 0 on area 1

4.3.Hypothesis 3. Height reduction in MI1, 4, 15, 16, 17, 18, MII5, 7, 10 and MII11.

The EVI conditions were already fulfilled for all the elements of the visual inventory except for area 1. In this new situation (see table 7), indicator a still remained greater than the initial value (0.2261 versus 0.1590) which led to the conclusion that the strategy of height reduction was definitely not effective enough.

More in detail, (see figure 7) the strategy was effective for the mitigation of visual effects in MI01, 04, 15, MII07, 10 and 11 but was not able to modify the effects of MI16, 17, 18 and MII05. That led to the rejection of the strategy of reduction of height and instead an attempt to use a technique of mitigation by vegetal barriers. This new decision left things as follows:

- Machines MI19, 20 and 21: definitely removed.
- The rest of WTs (31 machines): all of them repowered with WT model 2.

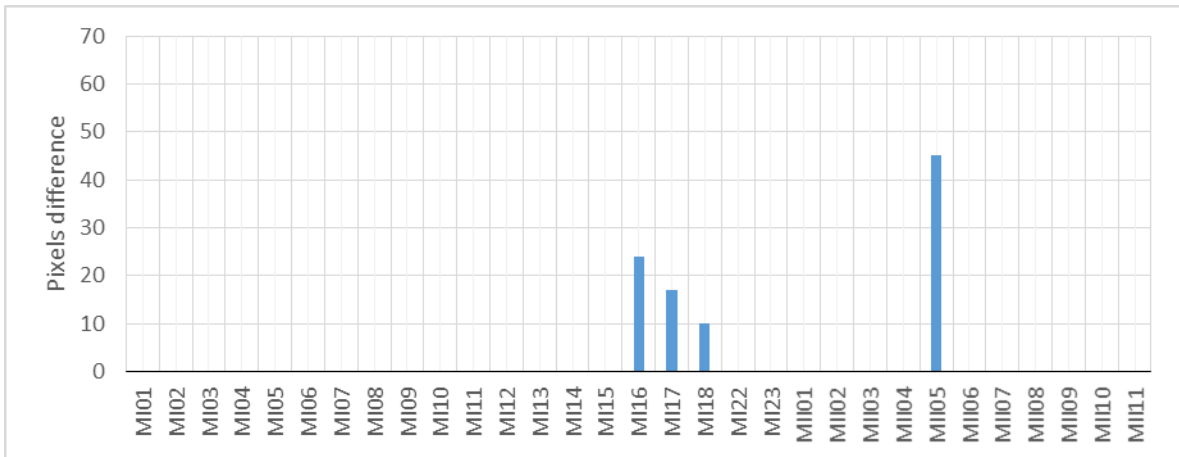


Figure 7: Comparative effect of the pixel difference between hypotheses 3 and 0 on area 1

4.4.Hypothesis 4. Mitigation by remote vegetation barrier.

This technique is based on a methodology that searches for those emplacements all over the area of study where erecting a strip of vegetation with a suitable height could provide the intended mitigation [1].

A vegetation barrier mitigation algorithm receives data including i) the DTM of the area of study, ii) the polygon whose visual intrusion must be mitigated (the area 1 in this case), iii) the values to delimit an acceptable solution (in general, not too close to the polygon, nor too close to the WF) and iv) the average barrier height. This latter was set to 25 meters (section 2.3). Several solutions were found (the problem could have had none), but only those that appeared in a type of soil categorised as forest were selected. Figure 8 shows the final solution that gave the best result in order to approach an EVI condition. Three different strips were found where a vegetal barrier could be effective: (i) barrier 1 mitigated WTs MI01 and MI04, (ii) a second one removed visual effects on WTs MII 7, 10, and MI15 and, (iii) finally, a third solved the problem for MII11, MII10 and MI15. Results appear in the corresponding row in table 7 (hypothesis 4, which achieves a value of 0.1894 for indicator α , was again still insufficient versus the original value of 0.1590).

Despite this, the situation described in figure 9 proves that hypothesis 4 was very efficient, enabling all the WTs in model 2 (31 units) to satisfy visual conditions, except for turbine MII05. Additionally, machines MI16 and MI17 showed a slight visual effect that was not relevant enough in the value of indicator α . WTs MI18, MII10 and MII11 in hypothesis 4 caused lesser visual effects than the ones in hypothesis 0.

All the previous effort led to a simple attempt: to act only on MII05, reducing its height. If this possibility failed, the designer would have the possibility of removing it. One way or the other, the repowering problem would be solved.

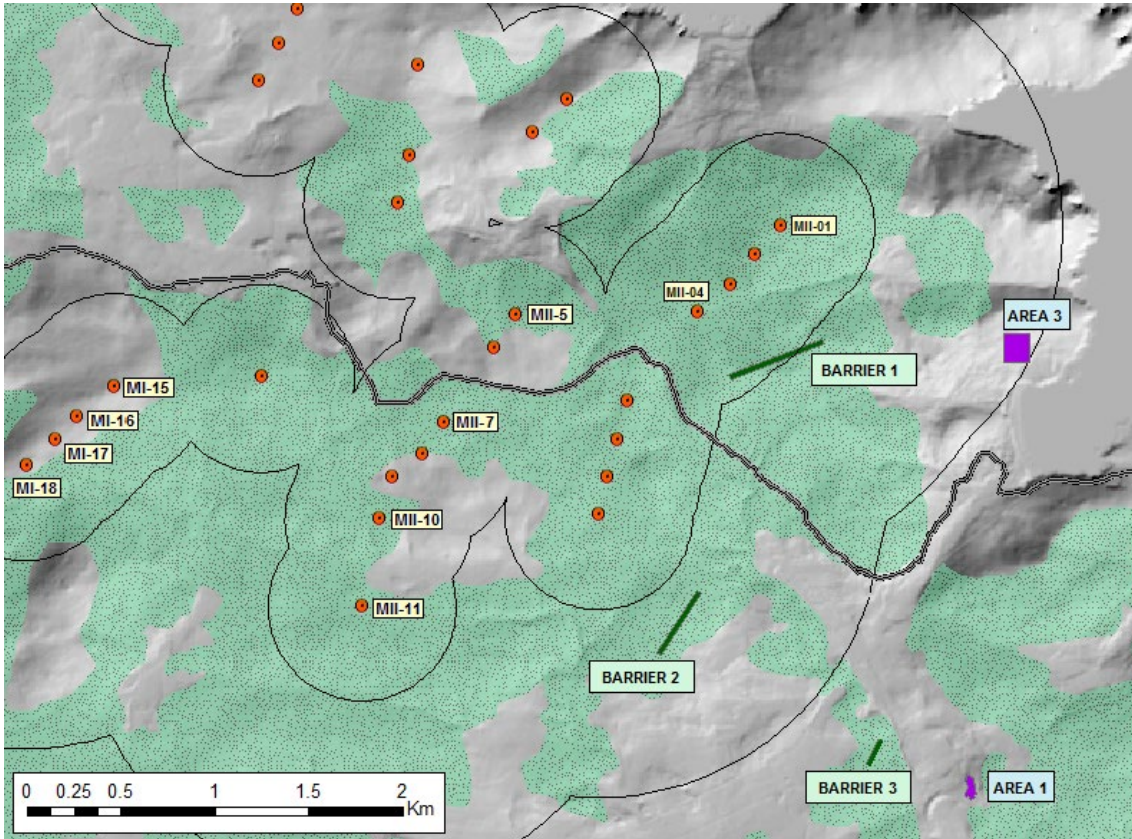


Figure 8: Location of the mitigation vegetation barriers (green strips). Dotted polygons correspond to forest areas. Only MII05 and wind turbines mitigated by vegetal barriers are labelled. Barrier 1 mitigates wind turbines MII01 and MII04. Barrier 2 affects visibility of MII07, 10 and MII15. Barrier 3 mainly mitigates MII11, but also affects MII10 and MII15.

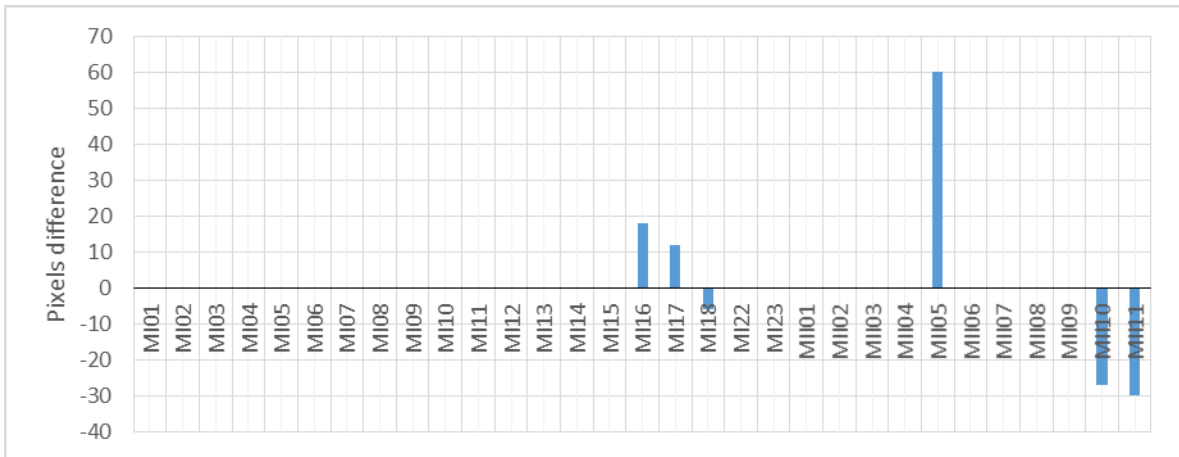


Figure 9: Comparative effect of the pixel difference between hypotheses 4 and 0 on area 1

4.5. Hypotheses 5 and 6. Reduction of the height of turbine MII05.

Assigning a height of 78 meters to WT MII05 (WT model 3, see section 2.4) led to obtaining a value of 0.1812 for indicator a (see hypothesis 5 in table 7), which was still insufficient. By again reducing MII05's height to 67 meters (model 4), indicator a in area 1 was 0.1564, which definitively provided a successful solution to the problem. Even though it is solved, figure 10

should be analysed because it helps in understanding that negative differences in WTs MI18, MII10 and MII11 help to reduce the overall value of indicator α , collaborating in this way to quicker convergence of the method to a successful solution.

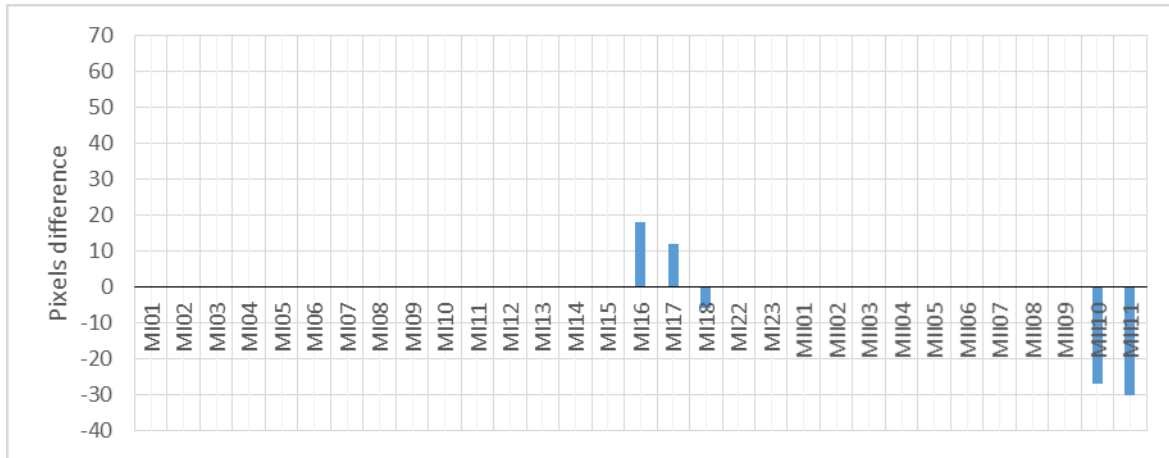


Figure 10: Comparative effect of the pixel difference between hypotheses 6 and 0 on area 1

In summary, the initial definition of thirty-four 67-meter-tall towers can be transformed into a new solution of thirty 93-meter-tall towers plus one more tower of 67 meters tall, together with three 25 m tall and 20 m wide vegetation strips: the longest one is 500 m, the next one is 400 m long and the shortest one is 140 m long. These barriers also fulfil the condition of being located in a type of soil categorised as forest, in which vegetation already exists, which facilitates their implementation and optimises cost (the solution might even consist simply of not cutting down the existing trees in those areas and letting them grow). The wind farm reconfiguration involves a repowering of 37.25% (77 MW versus its original value of 56.1 MW) assuring the EVI condition for both the overall and local effects in the visual inventory.

5. Discussion.

The EVI condition method needs neither a particular set of VIA indicators nor a particular set of visual inventory elements. These sets should be understood as degrees of freedom that should come from a stakeholder's agreement or an expert's decision.

The novelty of this procedure is twofold: on the one hand, visibility and Visual Impact are proved to be perfectly manageable criteria at the design stage of the WF; on the other hand, obtaining a sustainable design can be guided by an iterative process in which each hypothesis is formulated after a HRD analysis of the visual implications of the previous one.

The aforementioned analysis has been defined in section 3.4 and systematically applied in section 4. This analysis is the keystone of the procedure. Nonetheless, it currently has two drawbacks. The first one is that it does not provide control of convergence of the iteration: nothing guarantees the success in the series of decisions made, so that it can finish in a non-satisfactory solution (in fact this happened in section 4.3, leading to mitigation methods in section 3.4, which oriented the iteration towards the finally satisfactory solution). The second drawback is that we consider that the procedure should be automated, but we have not dealt with this task as yet. The rest of the elements (calculation of indicators, comparison between hypotheses and control of the visibility at a HRD) are already automated. In any case, the

decision itself to be made after each hypothesis is still dependent on the designer, not on the machine. This is not necessarily bad.

Other parts of the article, such as the reduced set of elements of the visual inventory and the short distance threshold (3500 m), require a brief comment. In regard to the reduced visual inventory, the method could be equally applied if we had had to analyse 30, 40 elements or more: in particular, the mitigation by vegetal barrier proves to be very efficient when applied to big sets of elements of the visual inventory.

Regarding the proposed distance threshold, it is short but gives rise to a domain larger than could have been envisaged initially (see figure 3). Anyway, we must say that in general short distance thresholds are a double-edged sword. It is true that in the field of Visual Impact Assessment, it is unusual to work with short visual effect distances but this also dramatically reduces the set of available mitigation measures (areas of vegetal barriers or new positions for some WTs) that the designer can propose, provided that they must be placed within this same territorial domain. In fact, this was more a hindrance than a help in this work.

6. Conclusion and future works.

This contribution should be understood as a way of including visibility and VIA criteria in the DSS (Decision Support System) applicable in the WF's design stage. Even though it is presented as a repowering problem, we have shown a methodology guided by VIA indicators that can be used to contrast different hypotheses of WF layouts and, what is more relevant, that is able to suggest new better ones based on the analysis of the visual implications. The methodology needs:

- A set of visual indicators. In our particular case, we selected two overall VIA indicators (creating the index MVE) and one local VIA indicator (the indicator α in SPM2).
- The idea of Equivalent Visual Impact (EVI) that states that two different layouts (in the same territory, having the same visual inventory) have EVI if the aforementioned set of indicators is individually equal. Setting a minimum value of tolerance is suggested.
- The need of processing visibility data at a High Resolution Data (HRD). This means providing visibility data at a pixel level and at a level of WT.

A study of the differences in visibility at a level of WT for two different hypotheses makes it possible to fine tune a third hypothesis, and so on until achieving the intended result. Nothing guarantees that there will always be a result (this is usually due to the terrain, not to the EVI method).

To finish, figure 11 is a concise summary of the case study developed in section 4. Blue columns show the evolution of the repowering hypotheses in terms of power (MW); brown columns show the evolution of the local visual resource consumed (magnified by a factor of 100 to be included appropriately in the same graph); grey lines show the efficiency of the repowering, it is the amount of power delivered by each unit of consumed visual resource (this ratio is magnified by a factor of 200 to be included in the same graph); yellow lines show the marginal VIA cost: the consumption of visual resource for one unit of generated power (in this case, the magnification factor is 10000). As a final reflection, this graph does not guarantee the acceptability of the solution obtained but clearly indicates the sustainability commitment with which it has been carried out. The graph itself is also a product of the methodology used.

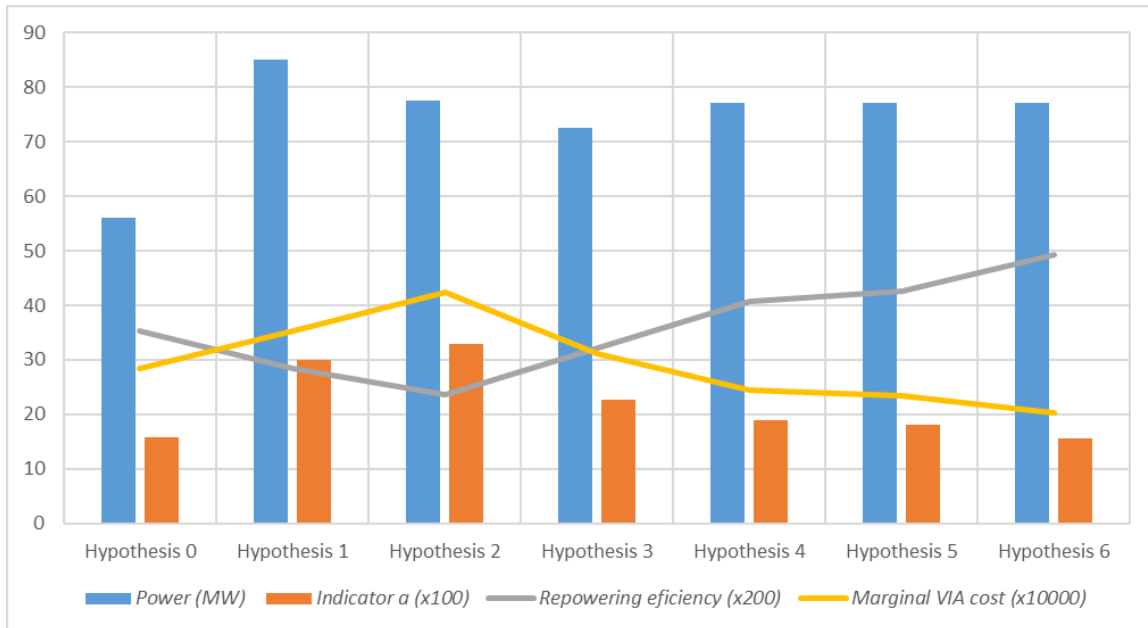


Figure 11: Comparison of the Visual cost for different analysed hypotheses. Differences in power (blue bars), indicator a (orange bars), repowering efficiency (grey line) and marginal VIA cost (yellow line).

Finally, future research is currently focused on two objectives: the first one is the computational optimization of the software that obtains the VIMs (see section 1.3); and the second one is the integration of such VIMs to the solving process exposed in this communication by means of optimization techniques.

References

- [1] Otero C, Manchado C, Arias R, Bruschi VM, Gomez-Jauregui V, Cendrero A. Wind energy development in Cantabria, Spain. Methodological approach, environmental, technological and social issues. *Renew Energ* 2012;40(1):137-149. Doi: 10.1016/j.renene.2011.09.008
- [2] Dirección General de Industria, Comercio y Consumo, Consejería de Innovación, Industria, Turismo y Comercio del Gobierno de Cantabria. Plan de Sostenibilidad Energética de Cantabria 2014-2020. Online: http://www.dgicc.cantabria.es/detalle/-/journal_content/56_INSTANCE_DETALLE/16626/2534689 (accessed July 2018. In spanish).
- [3] Hurtado JP, Fernandez J, Parrondo JL, Blanco E. Spanish method of visual impact evaluation in wind farms. *Renew Sust Energ Rev* 2004;8(5):483-491. Doi: 10.1016/j.rser.2003.12.009
- [4] Manchado C; Gomez-Jauregui V; Otero C. A review on the Spanish Method of visual impact assessment of wind farms: SPM2. *Renew Sust Energ Rev* 2015;49:756-767. Doi: 10.1016/j.rser.2015.04.067
- [5] Rodrigues M, Montañes C, Fueyo N. A method for the assessment of the visual impact caused by the large-scale deployment of renewable-energy facilities. *Environ Impact Assess* 2010;30(4):240-246. Doi: 10.1016/j.eiar.2009.10.004
- [6] Kokologos D, Tsitoura I, Louloupis V, Tsoutsos R. Visual impact assessment method for wind parks: A case study in Crete. *Land Use Policy* 2014;39:110-120. Doi: 10.1016/j.landusepol.2014.03.014

- [7] Tosoutsos T, Tsouchlaraki A, Tsiropoulos M, Serpetsidakis M. Visual impact evaluation of a wind park in a Greek island. *Appl Energy* 2009;86(4):546-553. Doi: 10.1016/j.apenergy.2008.08.013
- [8] McAulay IC. *Visual Descriptors: A Design Tool for Visual Impact Analysis*. University of Plymouth. Commissioning body, Faculty of Arts; 1988.
- [9] Bishop ID. Determination of Thresholds of Visual Impact: The Case of Wind Turbines. *Environ Plan B Urban Anal City Sci* 2002;29(5):707-718. Doi: 10.1068/b12854
- [10] Hagerhall CM; Purcell T; Taylor R. Fractal dimension of landscape silhouette outlines as a predictor of landscape preference. *J Environ Psychol* 2004;24(2):247-255. Doi: 10.1016/j.jenvp.2003.12.004
- [11] Bishop ID, Miller DR. Visual assessment of off-shore wind turbines: The influence of distance, contrast, movement and social variables. *Renew Energ* 2007;32(5):814-831. Doi: 10.1016/j.renene.2006.03.009
- [12] Ladenburg J, Dubgaard A. Willingness to pay for reduced visual disamenities from offshore wind farms in Denmark. *Energy Policy* 2007;35(8):4059-4071. Doi: 10.1016/j.enpol.2007.01.023
- [13] Ladenburg J. Visual impact assessment of offshore wind farms and prior experience. *Appl Energy* 2009;86(3):380-387. Doi: 10.1016/j.apenergy.2008.05.005.
- [14] Möller B. Changing wind-power landscapes: regional assessment of visual impact on land use and population in Northern Jutland, Denmark. *Appl Energy* 2006;83(5):477-494. Doi: 10.1016/j.apenergy.2005.04.004.
- [15] Torres-Sibille A, Cloquell-Ballester V, Cloquell-Ballester V, Darton R. Development and validation of a multicriteria indicator for the assessment of objective aesthetic impact of wind farms. *Renew Sust Energ Rev* 2009;13(1):40-66. Doi: 10.1016/j.rser.2007.05.002
- [16] Ladenburg J, Möller B. Attitude and acceptance of offshore wind farms-The influence of travel time and wind farm attributes. *Renew Sust Energ Rev* 2011;18(9):4223-4235. Doi: 10.1016/j.rser.2011.07.130
- [17] Molina-Ruiz J, Martinez-Sanchez MJ, Perez-Sirvent C, Tudela-Serrano ML, Garcia-Lorenzo ML. Developing and applying a GIS-assisted approach to evaluate visual impact in wind farms. *Renew Energ* 2011;36(3):1125-1132. Doi: 10.1016/j.eiar.2009.10.004.
- [18] Dentoni V, Massacci G. Assessment of visual impact induced by surface mining with reference to a case study located in Sardinia (Italy). *Environ Earth Sci* 2013;68(5):1485-1493. Doi: 10.1007/s12665-012-1994-3
- [19] Kapetanakis I, Kolokotsa D, Maria EA. Parametric analysis and assessment of the photovoltaics' landscape integration: Technical and legal aspects. *Renew Energ* 2014;67:207-214. Doi: 10.1016/j.renene.2013.11.043
- [20] Fernández-Jiménez LA, Mendoza-Villena M, Zorzano-Santamaría P, García-Garrido E, Lara-Santillán P, Zorzano-Alba E, Falces A. Site selection for new PV power plants based on their observability. *Renew Energ* 2017;75:7-15. Doi: 10.1016/j.renene.2014.12.063.
- [21] Wróżyński R, Sojka M, Pyszny K. The application of GIS and 3D graphic software to visual impact assessment of wind turbines. *Renew Energ* 2016;96:625-635. Doi: 10.1016/j.renene.2016.05.016.
- [22] Sunak Y, Madlener R. The impact of wind farm visibility on property values: A spatial difference-in-differences analysis. *Energy Econ* 2016;55:79-91. Doi: 10.1016/j.eneco.2015.12.025.
- [23] Ashuri T, Zaajier M.B, Martins J.R.R.A, van Bussel G.J.W, van Kuik G.A.M. Multidisciplinary design optimization of offshore wind turbines for minimum levelized cost of energy. *Renew Energ*, 2014;68:893–905. Doi: 10.1016/j.renene.2014.02.045.

- [24] Ashuri T, Zaajier M.B, Martins J.R.R.A, Zhang, J. Multidisciplinary design optimization of large wind turbines – Technical, economic, and design challenges. *Energy Convers Manag*, 2016;123:56–70. Doi: 10.1016/j.enconman.2016.06.004.
- [25] Serrano González J, González Rodríguez A.G, Castro Mora J, Riquelme Santos J, Burgos Payano M. Optimization of wind farm turbines layout using an evolutive algorithm. *Renew Energ*, 2010;35(8):1671–1681. Doi: 10.1016/j.renene.2010.01.010
- [26] Manchado C, Otero C, Gomez-Jauregui V, Arias R, Bruschi VM, Cendrero A. Visibility analysis and visibility software for the optimisation of wind farm design. *Renew Energ* 2013;60:388-401. Doi: 10.1016/j.renene.2013.05.026.
- [27] Otero C, Bruschi VM, Cendrero A, Galvez A, Lazaro M, Togoeres R. An Application of Computer Graphics for Landscape Impact Assessment, *Lect Notes Comput Sc* 2004:779-788. Doi: 10.1007/978-3-540-24709-8_82.
- [28] R&D EgiCAD, Universidad de Cantabria. MOYSES v4.0. Modeller and simulator for visual impact assessment. <http://193.144.189.246/moyses> (Accessed: December 2017).